# Diverse type VI secretion phospholipases are functionally plastic antibacterial effectors

**Alistair B. Russell**[1], **Michele LeRoux**[1,2], **Kristina Hathazi**[3,4], **Danielle M. Agnello**[1], **Takahiko Ishikawa**[3,4], **Paul A. Wiggins**[5,6], **Sun Nyunt Wai**[3,4], and **Joseph D. Mougous**[1,2,*]

[1]Department of Microbiology, University of Washington, Seattle, WA 98195, USA

[2]Molecular and Cellular Biology Program, University of Washington, Seattle WA 98195

[3]Department of Molecular Biology, Umeå University, SE-90187, Sweden

[4]The Laboratory for Molecular Infection Medicine Sweden (MIMS), Umeå University, SE-90187, Sweden

[5]Department of Physics, University of Washington, Seattle, WA 98195, USA

[6]Department of Bioengineering, University of Washington, Seattle, WA 98195, USA

## Abstract

Membranes allow the compartmentalization of biochemical processes and are therefore fundamental to life. The conservation of the cellular membrane, combined with its accessibility to secreted proteins, has made it a common target of factors mediating antagonistic interactions between diverse organisms. Here we report the discovery of a diverse superfamily of bacterial phospholipase enzymes. Within this superfamily, we defined enzymes with phospholipase A1 ($PLA_1$) and A2 ($PLA_2$) activity, which are common in host cell-targeting bacterial toxins and the venoms of certain insects and reptiles[1,2]. However, we find that the fundamental role of the superfamily is to mediate antagonistic bacterial interactions as effectors of the type VI secretion system (T6SS) translocation apparatus; accordingly, we name these proteins type VI lipase effectors (Tle). Our analyses indicate that PldA of *Pseudomonas aeruginosa*, a eukaryotic-like phospholipase D (PLD)[3], is a member of the Tle superfamily and the founding substrate of the haemolysin co-regulated protein secretion island II T6SS (H2-T6SS). While prior studies have specifically implicated PldA and the H2-T6SS in pathogenesis[3–5], we uncovered a specific role for the effector and its secretory machinery in intra- and inter-species bacterial interactions. Furthermore we find that this effector achieves its antibacterial activity by degrading phosphatidylethanolamine (PE), the major component of bacterial membranes. The surprising finding that virulence-associated phospholipases can serve as specific antibacterial effectors

*To whom correspondence should be addressed: J.D.M. -mougous@u.washington.edu.

suggests that interbacterial interactions are a relevant factor driving the ongoing evolution of pathogenesis.

Within proteobacterial genomes, predicted lipases are often encoded adjacent to homologs of the *vgrG* gene[6]. The VgrG protein is strongly associated with, and functionally important for, the cell contact-dependent T6S protein delivery pathway[7]. This pathway, which is distributed throughout all classes of Proteobacteria, can target both eukaryotic and bacterial cells; however, it is the specificity of its effectors that dictates the consequences of intoxication by the system. Known T6 effectors are few and include enzymes that either modify actin or degrade peptidoglycan – both domain-restricted molecules[8,9]. Thus, one would speculate that a barrier to the expansion or alteration of domain targeting would be the acquisition of a new effector or the evolution of one that is preexisting.

To understand the significance of the T6S-associated lipases we undertook an informatic approach to examine their genetic context, sequence, and phylogenetic distribution. This analysis uncovered 377 putative lipases comprising five divergent families (type VI lipase effector 1–5, Tle1-5) that share no detectable overall sequence homology (Fig. 1a and Supplementary Fig. 1–5). However, the families are united by a broad sporadic distribution pattern within Gram-negative bacteria and conserved putative catalytic motifs. Four of the families (Tle1-4) exhibit the GxSxG motif common in esterases and many lipases, while the fifth (Tle5) possesses dual HxKxxxxD motifs found in PLD enzymes (Fig. 1b)[1]. Outside of catalytic motifs, Tle1-4 members lack significant homology with known lipase enzymes, suggesting these proteins could represent previously uncharacterized diversity in the lipase superfamily.

Our prior work has shown that antibacterial T6S effectors are encoded adjacent to cognate immunity genes, which are essential due to the self-targeting activity of the T6S apparatus[9,10]. Moreover, due to a direct inactivation mechanism, the localization of the immunity protein indicates the cellular compartment targeted by the effector. Examination of the genomic context of the putative lipase-encoding genes revealed each is found adjacent to an open reading frame encoding a predicted periplasmic protein (Fig. 1a). Thus, we hypothesize that contrary to prevailing views of bacterial lipase function, *vgrG*-associated lipase families could universally serve roles in interbacterial competition, possibly targeting phospholipids accessible from the periplasm. Consistent with our hypothesis, one of the putative lipase enzymes that we identified, *V. cholerae* VC1418 (Tle2[VC], Supplementary Fig. 2), was recently found to act as an effector in amoeba defense and intraspecies bacterial competition[11]. Though the biochemical activity of Tle2[VC] was not elucidated, this suggests a capacity for Tle proteins to target a structure conserved in eukaryotes and bacteria.

To determine whether Tle2[VC] participates in interspecies bacterial antagonism, we tested its ability to provide fitness to *V. cholerae* in competition with *E. coli*. We observed *V. cholerae* strains lacking *tle2[VC]* display a striking impairment in their capacity to kill *E. coli*, approaching that of a strain lacking T6S function (Fig. 2a and Supplementary Fig. 6). It is of note that a prior study probing the function of Tle2[VC] did not observe a contribution of the protein to fitness in an interspecies setting[11]. This study was performed with strain V52, in which T6S-associated genes exhibit constitutively high expression[12]. Therefore, a potential

explanation for the apparent discrepancy is that in a hyperactive state the absence of one effector is not sufficient to diminish antibacterial activity to a measurable level.

Tle2 represents only one of four divergent GxSxG families within the broader superfamily. As a first step toward understanding the functional significance of other GxSxG families, we examined *B. thailandensis* BTH_I2698 (Tle1$^{BT}$, Fig. 1 and Supplementary Fig. 1), which we previously demonstrated to be a substrate of an antibacterial T6SS[10]. The *tle1$^{BT}$* gene is found adjacent to genes encoding two homologous periplasmic lipoproteins, I2699 and I2700, which we posited could serve as Tle1$^{BT}$ immunity proteins. Additionally, *tle1$^{BT}$*, I2699, and I2700 appear to have been subject to a duplication event, with homologs of all three genes present immediately upstream (Supplementary Fig. 7). To simplify our analysis, we generated a mutant strain lacking one copy of this duplicated region. Using labeled derivatives of this strain co-cultured under T6S-conducive conditions, we found that recipient strains lacking *tle1$^{BT}$* and its putative immunity determinants exhibit significantly decreased fitness in competition with donor strains possessing *tle1$^{BT}$* and a functional T6SS, and that expression of I2699 in the recipient strain was necessary and sufficient to restore competitive fitness (Fig. 2b). These data show that Tle1$^{BT}$ is an antibacterial effector delivered between cells by T6S, and that I2699, henceforth referred to as Tli1$^{BT}$ (type VI secretion lipase immunity 1), protects against Tle1$^{BT}$.

Having demonstrated that members of two GxSxG Tle families function as antibacterial T6S effectors, we next sought to investigate their biochemical activity. To characterize Tle1$^{BT}$ and Tle2$^{VC}$, we purified the proteins and catalytic nucleophile substitution mutant derivatives (Tle1$^{BT}$(S267A) and Tle2$^{VC}$(S371A)) as N-terminal fusions to hexahistidine-tagged maltose binding protein (MH–), which we found necessary to generate and maintain soluble protein (Supplementary Fig. 8 and 9). Importantly, Tle1-4 possess a Ser-Asp-His catalytic triad utilized by a diversity of esterase enzymes, including thioesterases, acetylesterases, and assorted lipase and phospholipases[1]. Given this wide range of potential activities, we initially confirmed general esterase activity of MH–Tle1$^{BT}$ and MH–Tle2$^{VC}$ by demonstrating that these effectors, but not their catalytic substitution mutants, hydrolyze a model substrate, polysorbate 20 (Supplementary Fig. 10). Next we asked whether MH–Tle1$^{BT}$ or MH–Tle2$^{VC}$ possess phospholipase activity. Using vesicle substrates doped with fluorescent phospholipid derivatives, we determined that MH–Tle1$^{BT}$ acts specifically as a PLA$_2$, and MH–Tle2$^{VC}$ as a PLA$_1$ (Fig. 2c,d). Linking these activities to the antibacterial phenotypes we observed associated with the proteins *in vivo*, neither Tle1$^{BT}$(S267A) nor Tle2$^{VC}$(S371A), both catalytically inactive, serve as antibacterial effectors (Fig. 2a,b). Moreover, we found that the PLA$_2$ activity of MH–Tle1$^{BT}$ is robustly inhibited by the addition of its immunity protein, Tli1$^{BT}$ (Fig. 2e).

If GxSxG family Tle proteins serve as antibacterial T6SS phospholipases, we reasoned that their activity against sensitive recipients should correlate with an increase in cellular permeability. To test these predictions, we performed single-cell measurements of propidium iodide (P.I.) uptake within interbacterial competitions of *B. thailandensis*. Consistent with our hypotheses, the lack of Tle1 immunity within cells corresponded to significantly increased P.I. uptake (Fig. 2f and Supplementary Videos 1–3). Using automated cell identity and tracking algorithms[13], we further demonstrated that the increase

in P.I. uptake depended upon direct contact with donor cells possessing a functional T6SS (Fig. 2g and Supplementary Fig. 11).

With our data validating members of two GxSxG families as antibacterial phospholipase effectors, we explored whether these findings could be extended to the HxKxxxxD family (Tle5). This catalytic motif is strongly indicative of PLD activity[1], which has heretofore not been associated with an antibacterial enzyme. We choose *P. aeruginosa* PldA, henceforth referred to as Tle5$^{PA}$ (Fig. 1 and Supplementary Fig. 5), as a representative Tle5 family member. We began our study by confirming the enzymatic activity of the protein, as its function was previously studied in the context of cellular extracts[3]. Consistent with prior observations, Tle5$^{PA}$ catalyzes the release of choline from phosphatidylcholine (PC), in a manner dependent upon a predicted catalytic histidine residue (His855) (Fig. 3a and Supplementary Fig. 12). Under similar conditions neither Tle1$^{BT}$ nor Tle2$^{VC}$ showed appreciable activity in this assay, underscoring the diverse substrate specificity within the Tle superfamily.

A candidate Tle5$^{PA}$ periplasmic immunity protein is not readily apparent, as the adjacent gene, PA3488, is predicted to encode a cytoplasmic protein. However, expression of PA3488 from a second, upstream, predicted start site yields a periplasmically-localized protein, henceforth referred to as Tli5$^{PA}$, that binds specifically to Tle5$^{PA}$ (Supplementary Fig. 13). To probe the role of Tle5$^{PA}$ and Tli5$^{PA}$ in interbacterial interactions, we generated a lysis reporter strain bearing a deletion of the *tle5$^{PA}$ tli5$^{PA}$* bicistron. Lysis of this strain was highly elevated when co-cultured with a wild-type, but not a *tle5$^{PA}$* donor strain (Fig. 3b). Additionally, expression of *tli5$^{PA}$* in the recipient was sufficient to protect from Tle5$^{PA}$-dependent lysis. Together, these data demonstrate Tle5$^{PA}$ acts as an antibacterial toxin and that Tli5$^{PA}$ is its cognate immunity determinant.

The *P. aeruginosa* genome encodes three T6SSs, the H1-3-T6SSs. The H1-T6SS is the only system with known substrates and a demonstrated role in interbacterial interactions[14]. To define the T6SS involved in Tle5$^{PA}$ transport, we constructed strains bearing individual in-frame deletions of the critical ATPase genes, *clpV1-3*, associated with the H1-3 systems, respectively. Specific inactivation of the H2-T6SS in a donor strain abrogated Tle5$^{PA}$-dependent toxicity, indicating that this system is responsible for Tle5$^{PA}$ delivery (Fig. 3b).

The finding that Tle5$^{PA}$ transits the H2-T6S pathway is interesting in light of data that implicate this T6SS as a virulence factor in plant, mammalian cell culture, worm, and mouse models of infection[4,5]. To more thoroughly explore the role of Tle5$^{PA}$ and the H2-T6SS in interbacterial interactions, we measured their influence on competition outcomes between *P. aeruginosa* and a model T6S target, *P. putida*[9]. Our results showed that both Tle5$^{PA}$ and the H2-T6SS significantly contribute to the fitness of *P. aeruginosa* in interspecies competition under T6S-conducive conditions (Fig. 3c and Supplementary Fig. 14). These findings show that Tle5$^{PA}$ is a potent antibacterial effector delivered by the H2-T6SS.

While our data thus far show that Tle1$^{BT}$, Tle2$^{VC}$, and Tle5$^{PA}$ possess phospholipase activity *in vitro*, this did not allow us to definitively assign the toxic consequences of these effectors to membrane destruction. The phospholipase activity of the effectors could be

accessory to a second toxicity mechanism found in these large, multidomain proteins. To resolve this remaining ambiguity concerning Tle function, we focused our studies on Tle5$^{PA}$. Since a mixture of healthy and intoxicated cells could complicate our measurements, we decided to assay Tle5$^{PA}$ effects in self-intoxicating monocultures of $tli5^{PA}$, wherein each cell serves both as a donor and a sensitive recipient. As expected, this strain exhibited increased membrane permeability in a manner dependent on an active H2-T6SS and Tle5$^{PA}$ (Supplementary Fig. 15).

Under conditions promoting intercellular delivery of Tle5$^{PA}$, we harvested lipids of both non-intoxicated (wild-type) and intoxicated ($tli5$) cells and quantified their phospholipid composition using mass spectrometry. This analysis revealed that the unchecked action of Tle5$^{PA}$ leads to a severely perturbed membrane phospholipid composition. Strikingly, phosphatidic acid (PA), a product of PLD activity and a minor constituent of wild-type membranes (0.17%), was present at 8.1% in $tli5^{PA}$ – a 48-fold enrichment (Fig. 3d and Supplementary Table 1). The increased PA appeared to derive primarily from PE, as it underwent a concomitant decrease of similar magnitude. Finally, we noted that phosphatidylglycerol (PG) increased slightly in $tli5$ relative to the wild-type. We speculate this latter result either derives from a compensatory effect or from Tle5$^{PA}$ activity against cardiolipin, a minor component of *P. aeruginosa* membranes not detectable by the analysis method we used. Taken together, these data strongly suggest that Tle5$^{PA}$-imposed cell death occurs through PA accumulation via PLD activity, primarily directed against PE. The precise physiological consequences of massive PA accumulation in bacterial cells are not known, however the strong negatively charged character of the molecule is likely to have a detrimental impact on both integral and peripheral membrane-associated proteins. It is known that PA induces membrane curvature that can promote fusion and fission events[15]; therefore, Tle5$^{PA}$ activity might also lead to generalized membrane destabilization, membrane blebbing and depolarization. Interestingly, the *in vivo* specificity of Tle5$^{PA}$ for PE, the major phospholipid constituent of most bacterial membranes, affords *P. aeruginosa* the capacity to use this enzyme against a vast array of competitors.

The discovery of T6SS-delivered phospholipase effectors has many implications. Critically, their biochemical activity does not intrinsically limit their toxicity to bacterial cells (Fig. 3e). Indeed, two specificities now ascribed to Tle superfamily members, PLD and PLA$_2$, are both highly represented in host cell-targeting bacterial toxins[2]. As these effectors are found in numerous established and emerging opportunistic pathogens, our work highlights the need to understand the biochemical, genetic, and evolutionary basis of inter-domain targeting by the T6SS. Such knowledge may ultimately become a component of a larger strategy to develop predictive algorithms for the evolution of bacterial pathogens. In addition, our findings add a new dimension to our understanding of the mechanisms employed during bacterial competition. Based on our data it appears that membrane targeting evolved independently on multiple occasions as an antibacterial strategy. This convergent evolution underscores the susceptibility of the bacterial membrane to attack, a theme mirrored by the prior observation that bacteriolytic T6S effectors likewise degrade an essential, conserved bacterial structure[9]. The continued discovery of antibacterial effectors

promises to illuminate additional vulnerabilities of the bacterial cell, and thus may aid our efforts to define promising therapeutic targets.

## Online-only Methods

### Bacterial strains and growth conditions

*B. thailandensis* strains used in this study were derived from the sequenced strain E264[16]. *B. thailandensis* strains were grown on either Luria-Bertani media (LB), or the equivalent lacking additional NaCl (LB low salt (LB-LS): 10 g bactopeptone and 5 g yeast extract per liter) at 37°C supplemented with 200 μg ml$^{-1}$ trimethoprim and 25 μg ml$^{-1}$ irgasan where necessary. For introducing in-frame deletions, *B. thailandensis* was grown on M9 minimal medium agar plates with 0.4% glucose as a carbon source and 0.1% (w/v) *p*-chlorophenylalanine for counter-selection[21]. *V. cholerae* strains used in this study were derived from the O1 El Tor strain A1552[18]. *V. cholerae* was grown on LB or LB with 340 nM NaCl at 37°C or 30°C supplemented with 100 μg/ml rifampin, 100μg/ml carbenicillin and stated concentrations of arabinose as needed. In order to introduce in-frame deletions *V. cholerae* was grown on LB supplemented with 10% (w/v) sucrose at 30 °C for counter-selection[22,23]. *P. aeruginosa* strains used in this study were derived from the sequenced strain PAO1[17]. *P. aeruginosa* strains were grown on LB at 37 °C supplemented with 25 μg ml$^{-1}$ irgasan, 30 μg ml$^{-}$ gentamycin, and stated concentrations of IPTG as required. To generate in-frame deletions *P. aeruginosa* was grown on LB-LS supplemented with 5% (w/v) sucrose at 30 °C for counter-selection[24]. For intra- and inter-species competition *P. aerguinosa* was grown on synthetic cystic fibrosis sputum media (SCFM) at 23°C[19]. *P. putida* used in this study was the sequenced strain, KT2440[25]. *P. putida* was grown on LB at 30°C or on SCFM at 23°C. *E. coli* strains included in this study included DH5α for plasmid maintenance and production of Tli1$^{BT}$ immunoprecipitate, SM10 λ*pir* for conjugal transfer of plasmids into *B. thailandensis*, *V. cholerae,* and *P. aeruginosa*, MC4100 for competition assays with *V. cholerae,* BL21(DE3) p*lysS* for Tle5$^{PA}$ immunoprecipitation studies, and Shuffle T7 p*lysY* Express(New England Biolabs), for purification of Tle proteins. All *E. coli* strains were grown on LB or 2xYT at 37 °C supplemented with 150 μg ml$^{-1}$ carbenicillin, 50 μg ml$^{-1}$ kanamycin, 30 μg ml$^{-1}$ chloramphenicol, 200 μg ml$^{-1}$ trimethoprim, 50μg/ml streptomycin, 15μg/ml gentamycin, 0.1% rhamnose, and 100 mM IPTG as needed.

### DNA manipulations

The creation, maintenance, and transformation of plasmid constructs followed standard molecular cloning procedures. All primers used in this study were obtained from Integrated DNA Technologies. DNA amplification was carried out using either Phusion (New England Biolabs) or Mangomix (Bioline). DNA sequencing was performed by Genewiz Incorporated. Restriction enzymes were obtained from New England Biolabs. SOE PCR was performed as previously described[26].

### Plasmid construction

Plasmids used for expression in this study were pET28b:His$_6$-MBP-TEV-His$_6$[27], pET22b+ (Novagen), and pSCrhaB2[28] for *E. coli*, pPSV35CV[29] for *P. aeruginosa*, and pBAD24[30] for *V. cholerae*. Complementation in *B. thailandensis* was performed using the Tn7-based

integration vector pUC18T-miniTn7T-Tp::PS12[31]. In-frame deletions were generated utilizing the suicide vectors pJRC115 for *B. thailandensis*[21], pVCD442 for *V. cholerae*[32], and pEXG2 for *P. aeruginosa*[24]. For the production of deletion constructs either 600 bp (*B. thailandensis* and *P. aeruginosa*) or 500 bp (*V. cholerae*) regions flanking the deletion were amplified, ligated together using SOE PCR, and subsequently cloned into pJRC115, pEXG2, or pVCD442 respectively. To generate the $tle1^{BT}_{S267A}$ *B. thailandensis* mutation construct, 600 bp regions flanking the mutation with an additional overlapping extension consisting of the desired mutation were amplified and ligated together using SOE PCR and subsequently cloned into pJRC115. For *B. thailandensis* complementation constructs genes were amplified along with predicted ribosomal-binding sites and cloned into pUC18T-miniTn7T-Tp::P12. For *P. aeruginosa* complementation and expression constructs, genes were amplified with their native ribosomal binding sites into pPSV35CV with a 3′ fusion to the VSV–G (vesicular stomatitis virus glycoprotein) epitope tag. To further generate the pPSV35CV::$tle5^{PA}_{H167R}$ and $_{H855R}$–V constructs, the entire $tle5^{PA}$ gene was amplified from pPSV35CV::$tle5^{PA}$ and SOE PCR was used to introduce the desired base pair mutations. For pSCrhaB2 *E. coli* expression constructs and pBAD24 *V. cholerae* expression and complementation constructs, genes were cloned downstream of the optimized ribosomal binding site already present in these vectors with a fusion to a 3′ VSV–G-linker. To further generate the pBAD24::$tle2^{VC}_{S371A}$–V construct, the entire $tle2^{VC}$ gene was amplified from pBAD24::$tle2^{VC}$–V and SOE PCR was used to introduce the desired base pair mutations. This product was subsequently cloned into pBAD24. For the Tle purification constructs *tle* genes were amplified and cloned into pET28b:His$_6$-MBP-TEV-His$_6$ to generate an N-terminal fusion to an MBP protein and a hexahistidine purification tag. SOE PCR was then used to generate the desired catalytic nucleophile substitution mutants. For the Tle5$^{PA}$ periplasmic expression construct, $tle5^{PA}$ was amplified and cloned into pET22b+ to generate an N-terminal fusion to the PelB leader peptide and a C-terminal fusion to a hexahistidine epitope tag.

### Informatic identification of Tle proteins

All sequences were obtained from NCBI (http://www.ncbi.nlm.nih.gov), and Genbank accession numbers for all Tle proteins identified in this study are found in Supplementary Fig. 1–5. BTH_I2698 from *B. thailandensis* E264, PA0260, PA1510, PA3487, and PA5089 from *P. aeruginosa* PAO1, and VC1418 from *V. cholerae* V52, all encoded adjacent to *vgrG* genes, were identified as putative lipases utilizing the PHYRE 2 structural prediction server[33]. Using the amino acid sequences of these predicted lipases, blastp analyses were performed against the non-redundant protein database (ftp://ftp.ncbi.nih.gov/blast/db/) to identify unique instances of their homologs. Homology identified by the blast server was used to distribute these proteins into five distinct Tle families. Each family was aligned using the MUSCLE algorithm and phylogenetic trees were generated using the PHYML 3.0 method with bootstrap analysis of 1000 replicates[34,35]. Proteins encoded by the genes shown in Figure 1a were analyzed for subcellular localization utilizing the SignalP 3.0 and TMHMM 2.0 servers, and VgrG proteins were identified utilizing blastp[36,37]. Regions depicted in Figure 1a were extracted based on boundaries defined by the presence of a *tle*, *tli*, or *vgrG* gene. Fig. 1b catalytic residues were determined both by PHYRE 2 structural alignment with known lipase enzymes and conservation of those residues within the Tle

family alignments. Sequence logos were generated from a manual alignment of conserved catalytic motifs utilizing Geneious software.

## Western blot analyses

Whole cell fractions were prepared as described previously[29]. Anti-RNA polymerase, anti-VSV–G, anti-beta-lactamase, anti-His$_5$, and anti-CRP Western blot analyses were performed utilizing previously-defined methods[9,23,38]. To analyze the expression of epitope-tagged Tle2$^{VC}$ and Tle2$^{VC}_{S371A}$ in *V. cholerae*, cells were grown in LB medium at 37 °C to an optical density at 600 nm (OD$_{600}$) of 0.5, induced with 0.0002% (w/v) arabinose, and then harvested at a final OD$_{600}$ of 2.0. To analyze the expression of epitope-tagged Tle5$^{PA}$, Tle5$^{PA}_{H167R}$, and Tle5$^{PA}_{H855R}$, in *P. aeruginosa*, cells were grown in LB medium supplemented with 1mM IPTG at 37 °C and harvested at an OD$_{600}$ of 1.0. Subcellular localization of epitope-tagged Tle1$^{PA}$ and Tli1$^{PA}$ in *P. aeruginosa* was performed identically to previous localization studies of Tsi1 and Tsi3[9,39]. For immunoprecipitation experiments, BL21(DE3) p*lysS* cells co-expressing periplasmic hexahistidine-tagged Tle5$^{PA}$ from a pet22b+ vector and VSV–G tagged immunity proteins from pSCrhaB2 vectors were pelleted and resuspended in lysis buffer (20 mM Tris-Cl pH 7.5, 50 mM KCl, 8.0% (v/v) glycerol, 1.0% (v/v) triton, supplemented with DNase I (Roche), lysozyme (Roche), and 200μM PMSF). Cells were disrupted by sonication and the solution clarified by centrifugation. A sample of supernatant was then taken for analysis of total protein. The remainder of the supernatant was incubated with anti-VSV–G agarose beads (Sigma) for 1 h at 4°C. Beads were washed four times with IP-wash buffer (100 mM NaCl, 25 mM KCl, 0.1% (v/v) triton, 20 mM Tris-Cl pH 7.5, and 2% (v/v) glycerol). Proteins were removed from beads with SDS loading buffer (125 mM Tris, pH6.8, 2% (w/v) 2-mercaptoethanol, 20% (v/v) glycerol, 0.001% (w/v) bromophenol blue and 4% (w/v) SDS) and analyzed by Western blot.

## Bacterial competition experiments

Burkholderia competition experiments were performed as described previously[10]. Recipient strains (Fig. 2b, left), or donor strains (Fig. 2b, right) were labeled with a GFP-expression constructed integrated into the attTn7 site, allowing the disambiguation of donor and recipient colonies through fluorescence imaging[40]. For *V. cholerae* competition experiments with *E. coli*, both strains were grown to an OD$_{600}$ of 0.5 in LB before being mixed 1:1 by volume. This mixture was then spotted on a nitrocellulose membrane on a 1.5% (w/v) agar LB plate containing 300 mM NaCl and 0.002% (w/v) arabinose. Competitions were incubated for 5 h at 37°C. Cells were then harvested and competitions analyzed. Initial and final colony-forming units (CFUs) of *V. cholerae* and *E. coli* were enumerated on LB plates supplemented with rifampin and streptomycin respectively. For *P. aeruginosa* competitions with *P. putida*, strains were grown overnight on solid LB media at 37 °C (*P. aeruginosa*) or 30 °C (*P. putida*) and resuspended in water to an OD$_{600}$ of 0.3. Cells were mixed 1:1 and spotted on 1.5% (w/v) agar SCFM media plates, or inoculated into liquid media of the same. After 23 h of incubation at 23°C, a temperature previously demonstrated conducive to H2-T6SS and Tle5$^{PA}$ expression under *in vitro* conditions[41], cells were harvested and relative numbers of bacteria determined. Both initial and final counts of *P. aeruginosa* and *P. putida* were determined by plate counts. *P. aeruginosa* self-intoxication assays were performed

under identical conditions to solid media competition assays, save for the addition of 1 mM IPTG. After 23 h of growth, cells were stained with 5 μg ml$^{-1}$ propidium iodide in PBS pH 7.0 for 10 minutes and washed prior to fluorescence measurements at an excitation/emission of 535/617 nm. Values shown were corrected for cellular density as measured by OD$_{600}$. Competition results for *B. thailandensis* and *P. aeruginosa* experiments are the change in ratio of donor cells to recipient cells, competition results from *V. cholerae* represent the final ratio alone. Data from all competitions were analyzed by a two-tailed Student's T-test, and data from monoculture experiments were analyzed by a one-tailed Student's T-test for a significant increase in P.I. staining.

### Enzymatic assays of lipase activity

The hydrolysis of polysorbate 20 was measured as described by Tigerstrom and Stelmaschuk[42]. These experiments were performed at 28°C at a final enzyme concentration of 60 nM in a buffer consisting of 20 mM Tris-Cl pH 7.2, 100 mM NaCl, 3 mM CaCl$_2$ and 2% (v/v) polysorbate 20. Fluorescence assays for phospholipase A activity were performed utilizing PED-A1 (*sn1*-labeled) and PED6 (*sn2*-labeled) fluorescent substrates according to manufacturer's directions (Invitrogen). Activity of Tle1$^{PA}$ and Tle2$^{VC}$ on these substrates was measured at an enzyme concentration of 300 nM (Tle1$^{PA}$) or 30 nM (Tle2$^{VC}$) at 28°C. For Tle1$^{BT}$-inhibition assays, immunoprecipitate was obtained as detailed under Western blot analyses from *E. coli* DH5α bearing a pSCrhaB2::*tli1$^{BT}$*–V expression construct or the equivalent empty vector control, with the modification that proteins were eluted from anti-VSV–G agarose beads by the addition of VSV–G peptide at a concentration of 100 μg ml$^{-1}$ and no PMSF was used. After the addition of immunoprecipitate to Tle1$^{BT}$ enzymatic reactions, samples were incubated for four minutes after which the first reading was normalized to the measurement immediately prior to treatment. Fluorescent assays for phospholipase D activity were performed by measuring the production of peroxide by choline oxidase through the generation of the fluorescent molecule resorufin from Amplex red reagent (Invitrogen) according the manufacturer's directions with the following modifications: reactions were performed in a buffer consisting of 50 mM Tris-Cl pH 7.2, 100 mM NaCl, 5 mM CaCl$_2$, and 2 mM MgCl$_2$, and vesicles consisting of equal amounts dioleoylphosphatidylcholine and dioleoylphosphatidylglycerol were used as a substrate at a final reaction concentration of 16.7 μM for each lipid species. Activity was measured at an enzyme concentration of 130 nM at 28°C. In all assays fluorescent values were corrected for fluorescence as measured in a buffer-only control.

### Competitive lysis assays

The lysis of *P. aeruginosa* reporter strains was determined by the relative partitioning of LacZ to the supernatant. Lysis reporter strains were generated by the chromosomal integration of a previously-described miniCTX vector containing *lacZ* under the expression of a constitutive promoter[43]. Lysis reporter strains and unmarked donor strains were grown overnight on solid LB media at 37°C and then resuspended in water to an OD$_{600}$ of 0.3. Donor and recipient strains were mixed 1:1 and spotted on 1.5% (w/v) agar SCFM plates supplemented with 1 mM IPTG and incubated at 23°C for 23 h. Relative levels of supernatant LacZ activity as compared to total LacZ activity were then determined as previously described[20]. Data were analyzed using a two-tailed Student's T-test.

## Microscopic analyses of interbacterial competitions

Time-lapse fluorescence microscopy sequences were acquired with a Nikon Ti-E inverted microscope fitted with a 60X oil objective, automated focusing (Perfect Focus System, Nikon), a Xenon light source (Sutter Instruments), a CCD camera (Clara series, Andor), and a custom environmental chamber. NIS Elements (Nikon) was used for automated image acquisition. Overnight cultures of recipient (*B. thailandensis* ΔBTH_I2698-I2703 attTn7::*gfp*) and donor (either *B. thailandensis* wild-type, ΔBTH_I2698 ΔBTH_I2701-3, or ΔBTH_I2598) strains were mixed 1:1 and diluted 2-fold with LB. The resulting bacterial suspension (~2 μL) was spotted onto growth pads made with LB broth, 2.5% (w/v) agarose, 0.2% (w/v) sodium nitrate, and 2.5 μg mL$^{-1}$ propidium iodide. Automated image acquisition was performed at 5-min intervals for 6–8 h at 30°C. Cell identification, cell linking, and donor-contact analyses were performed using customized Matlab-based software (2012a, Mathworks) as described previously[13]. Donor (unlabeled) and recipient (GFP-labeled) populations were identified using an empirically determined green fluorescence gate. A P.I. uptake event was defined as the first frame in which a cell achieved an empirically determined mean red fluorescence intensity threshold. Counting error was calculated as the square root of measurable events. Results represent two fields of view from a single experiment; each experiment was independently repeated at least three times. Videos generated from cropped regions of the three growth competition experiments depicted are provided (Supplementary Videos 1–3).

## Protein purification

For purification, Tle proteins were expressed from pET28b:His$_6$-MBP-TEV-His$_6$ in Shuffle T7 pLysY Express cells (New England Biolabs). Proteins were purified to homogeneity using nickel chromatography followed by size-exclusion chromatography using previously-reported methods, with the exception that reducing agents were excluded[44].

## Lipidomic analyses

Wild-type and *tli5* mutant *P. aerguinosa* strains were grown as 20 individual 10 μl spots on 1.5 % (w/v) agar SCFM plates for 23 h at 23°C. These spots were then resuspended in PBS and lipids were extracted using the Bligh-Dyer method[45]. Purified lipid samples were analyzed for PE, PC, PG, and PA content by the Kansas State Lipidomics Research Center. An automated electrospray ionization-tandem mass spectrometry approach was used, and data acquisition and analysis were carried out as described previously[46,47] with modifications. The lipid samples were dissolved in 1 ml chloroform. An aliquot of 50 μl of extract in chloroform was used. Precise amounts of internal standards, obtained and quantified as previously described[48], were added in the following quantities (with some small variation in amounts in different batches of internal standards): 0.6 nmol di12:0-PC, 0.6 nmol di24:1-PC, 0.6 nmol 13:0-lysoPC, 0.6 nmol 19:0-lysoPC, 0.3 nmol di12:0-PE, 0.3 nmol di23:0-PE, 0.3 nmol 14:0-lysoPE, 0.3 nmol 18:0-lysoPE, 0.3 nmol di14:0-PG, 0.3 nmol di20:0(phytanoyl)-PG, 0.3 nmol di14:0-PA, and 0.3 nmol di20:0(phytanoyl)-PA. The sample and internal standard mixture was combined with solvents, such that the ratio of chloroform/methanol/300 mM ammonium acetate in water was 300/665/35, and the final volume was 1.4 ml. Unfractionated lipid extracts were introduced by continuous infusion

into the ESI source on a triple quadrupole MS/MS (4000QTrap), Applied Biosystems, Foster City, CA). Samples were introduced using an autosampler (LC Mini PAL, CTC Analytics AG, Zwingen, Switzerland) fitted with the required injection loop for the acquisition time and presented to the ESI needle at 30 μl/min. Sequential precursor and neutral loss scans of the extracts produce a series of spectra with each spectrum revealing a set of lipid species containing a common head group fragment. Lipid species were detected with the following scans: PC and lysoPC, $[M + H]^+$ ions in positive ion mode with Precursor of 184.1 (Pre 184.1); PE and lysoPE, $[M + H]^+$ ions in positive ion mode with Neutral Loss of 141.0 (NL 141.0); PG, $[M + NH_4]^+$ in positive ion mode with NL 189.0 for PG; and PA, $[M + NH_4]^+$ in positive ion mode with NL 115.0. The collision gas pressure was set at 2 (arbitrary units). The collision energies, with nitrogen in the collision cell, were +28 V for PE, +40 V for PC, +25 V for PA, and +20 V for PG. . Declustering potentials were +100 V for all lipids. Entrance potentials were +15 V for PE and +14 V for PC, PA, and PG. Exit potentials were +11 V for PE and +14 V for PC, PA, and PG. The scan speed was 50 or 100 u per sec. The mass analyzers were adjusted to a resolution of 0.7 u full width at half height. For each spectrum, 9 to 150 continuum scans were averaged in multiple channel analyzer (MCA) mode. The source temperature (heated nebulizer) was 100 °C, the interface heater was on, +5.5 kV were applied to the electrospray capillary, the curtain gas was set at 20 (arbitrary units), and the two ion source gases were set at 45 (arbitrary units). The background of each spectrum was subtracted, the data were smoothed, and peak areas integrated using a custom script and Applied Biosystems Analyst software, and the data were isotopically deconvoluted. The first set of mass spectra were acquired on the internal standard mixture only. Peaks corresponding to the target lipids in these spectra were identified and molar amounts calculated in comparison to the two internal standards on the same lipid class. To correct for chemical or instrumental noise in the samples, the molar amount of each lipid metabolite detected in the "internal standards only" spectra was subtracted from the molar amount of each metabolite calculated in each set of sample spectra. The data from each "internal standards only" set of spectra was used to correct the data. Values expressed are the percentage of the total polar lipid signal detected. Statistical significance analyzed by a two-tailed Student's T-test.

## Supplementary Material

Refer to Web version on PubMed Central for supplementary material.

## Acknowledgments

# References

1. Aloulou A, Ali YB, Bezzine S, Gargouri Y, Gelb MH. Phospholipases: an overview. Methods in Molecular Biology. 2012; 861:63–85. [PubMed: 22426712]

2. Schmiel DH, Miller VL. Bacterial phospholipases and pathogenesis. Microbes and infection / Institut Pasteur. 1999; 1:1103–1112. [PubMed: 10572314]

3. Wilderman PJ, Vasil AI, Johnson Z, Vasil ML. Genetic and biochemical analyses of a eukaryotic-like phospholipase D of Pseudomonas aeruginosa suggest horizontal acquisition and a role for persistence in a chronic pulmonary infection model. Molecular microbiology. 2001; 39:291–303. [PubMed: 11136451]

4. Lesic B, Starkey M, He J, Hazan R, Rahme LG. Quorum sensing differentially regulates Pseudomonas aeruginosa type VI secretion locus I and homologous loci II and III, which are required for pathogenesis. Microbiology (Reading, England). 2009; 155:2845–2855.

5. Sana TG, et al. The second type VI secretion system of Pseudomonas aeruginosa strain PAO1 is regulated by quorum sensing and Fur and modulates internalization in epithelial cells. The Journal of biological chemistry. 2012; 287:27095–27105. [PubMed: 22665491]

6. Barret M, Egan F, Fargier E, Morrissey JP, O'Gara F. Genomic analysis of the type VI secretion systems in Pseudomonas spp.: novel clusters and putative effectors uncovered. Microbiology (Reading, England). 2011; 157:1726–1739.

7. Silverman JM, Brunet YR, Cascales E, Mougous JD. Structure and Regulation of the Type VI Secretion System. Annual review of microbiology. 2012; 66:453–473.

8. Pukatzki S, Ma AT, Revel AT, Sturtevant D, Mekalanos JJ. Type VI secretion system translocates a phage tail spike-like protein into target cells where it cross-links actin. Proc Natl Acad Sci U S A. 2007; 104:15508–15513. [PubMed: 17873062]

9. Russell AB, et al. Type VI secretion delivers bacteriolytic effectors to target cells. Nature. 2011; 475:343–347. [PubMed: 21776080]

10. Russell AB, et al. A widespread bacterial type VI secretion effector superfamily identified using a heuristic approach. Cell host & microbe. 2012; 11:538–549. [PubMed: 22607806]

11. Dong TG, Ho BT, Yoder-Himes DR, Mekalanos JJ. Identification of T6SS-dependent effector and immunity proteins by Tn-seq in Vibrio cholerae. Proceedings of the National Academy of Sciences of the United States of America. 2013; 110:2623–2628. [PubMed: 23362380]

12. Ishikawa T, et al. Pathoadaptive conditional regulation of the type VI secretion system in Vibrio cholerae O1 strains. Infection and immunity. 2011; 80:575–584. [PubMed: 22083711]

13. Leroux M, et al. Quantitative single-cell characterization of bacterial interactions reveals type VI secretion is a double-edged sword. Proceedings of the National Academy of Sciences of the United States of America. 2012; 109:19804–19809. [PubMed: 23150540]

14. Mougous JD, et al. A virulence locus of Pseudomonas aeruginosa encodes a protein secretion apparatus. Science. 2006; 312:1526–1530. [PubMed: 16763151]

15. Stace CL, Ktistakis NT. Phosphatidic acid- and phosphatidylserine-binding proteins. Biochimica et biophysica acta. 2006; 1761:913–926. [PubMed: 16624617]

16. Kim HS, et al. Bacterial genome adaptation to niches: divergence of the potential virulence genes in three Burkholderia species of different survival strategies. BMC genomics. 2005; 6:174. [PubMed: 16336651]

17. Stover CK, et al. Complete genome sequence of Pseudomonas aeruginosa PA01, an opportunistic pathogen. Nature. 2000; 406:959–964. [PubMed: 10984043]

18. Yildiz FH, Schoolnik GK. Role of rpoS in stress survival and virulence of Vibrio cholerae. Journal of bacteriology. 1998; 180:773–784. [PubMed: 9473029]

19. Palmer KL, Aye LM, Whiteley M. Nutritional cues control Pseudomonas aeruginosa multicellular behavior in cystic fibrosis sputum. J Bacteriol. 2007; 189:8079–8087. [PubMed: 17873029]

20. Chou S, et al. Structure of a Peptidoglycan Amidase Effector Targeted to Gram-Negative Bacteria by the Type VI Secretion System. Cell Rep. 2012; 1:656–664. [PubMed: 22813741]

21. Chandler JR, et al. Mutational analysis of Burkholderia thailandensis quorum sensing and self-aggregation. J Bacteriol. 2009; 191:5901–5909. [PubMed: 19648250]

Author Manuscript

22. Vaitkevicius K, et al. A Vibrio cholerae protease needed for killing of Caenorhabditis elegans has a role in protection from natural predator grazing. Proceedings of the National Academy of Sciences of the United States of America. 2006; 103:9280–9285. [PubMed: 16754867]

23. Valeru SP, et al. Role of melanin pigment in expression of Vibrio cholerae virulence factors. Infection and immunity. 2009; 77:935–942. [PubMed: 19103773]

24. Rietsch A, Vallet-Gely I, Dove SL, Mekalanos JJ. ExsE, a secreted regulator of type III secretion genes in Pseudomonas aeruginosa. Proc Natl Acad Sci U S A. 2005; 102:8006–8011. [PubMed: 15911752]

25. Nelson KE, et al. Complete genome sequence and comparative analysis of the metabolically versatile Pseudomonas putida KT2440. Environmental microbiology. 2002; 4:799–808. [PubMed: 12534463]

26. Horton RM, et al. Gene splicing by overlap extension. Methods in enzymology. 1993; 217:270–279. [PubMed: 8474334]

27. Korotkov KV, Hol WG. Crystal structure of the pilotin from the enterohemorrhagic Escherichia coli type II secretion system. J Struct Biol. 2013

28. Cardona ST, Valvano MA. An expression vector containing a rhamnose-inducible promoter provides tightly regulated gene expression in Burkholderia cenocepacia. Plasmid. 2005; 54:219–228. [PubMed: 15925406]

29. Hsu F, Schwarz S, Mougous JD. TagR promotes PpkA-catalysed type VI secretion activation in Pseudomonas aeruginosa. Mol Microbiol. 2009; 72:1111–1125. [PubMed: 19400797]

30. Guzman LM, Belin D, Carson MJ, Beckwith J. Tight regulation, modulation, and high-level expression by vectors containing the arabinose PBAD promoter. Journal of bacteriology. 1995; 177:4121–4130. [PubMed: 7608087]

31. Schell MA, et al. Type VI secretion is a major virulence determinant in Burkholderia mallei. Mol Microbiol. 2007; 64:1466–1485. [PubMed: 17555434]

32. Donnenberg MS, Kaper JB. Construction of an eae deletion mutant of enteropathogenic Escherichia coli by using a positive-selection suicide vector. Infection and immunity. 1991; 59:4310–4317. [PubMed: 1937792]

33. Kelley LA, Sternberg MJ. Protein structure prediction on the Web: a case study using the Phyre server. Nature protocols. 2009; 4:363–371. [PubMed: 19247286]

34. Edgar RC. MUSCLE: multiple sequence alignment with high accuracy and high throughput. Nucleic acids research. 2004; 32:1792–1797. [PubMed: 15034147]

35. Guindon S, et al. New algorithms and methods to estimate maximum-likelihood phylogenies: assessing the performance of PhyML 3.0. Systematic biology. 2010; 59:307–321. [PubMed: 20525638]

36. Bendtsen JD, Nielsen H, von Heijne G, Brunak S. Improved prediction of signal peptides: SignalP 3.0. J Mol Biol. 2004; 340:783–795. [PubMed: 15223320]

37. Emanuelsson O, Brunak S, von Heijne G, Nielsen H. Locating proteins in the cell using TargetP, SignalP and related tools. Nature protocols. 2007; 2:953–971. [PubMed: 17446895]

38. Balsalobre C, et al. Release of the type I secreted alpha-haemolysin via outer membrane vesicles from Escherichia coli. Molecular microbiology. 2006; 59:99–112. [PubMed: 16359321]

39. Imperi F, et al. Analysis of the periplasmic proteome of Pseudomonas aeruginosa, a metabolically versatile opportunistic pathogen. Proteomics. 2009; 9:1901–1915. [PubMed: 19333994]

40. Schwarz S, et al. Burkholderia type VI secretion systems have distinct roles in eukaryotic and bacterial cell interactions. PLoS Pathog. 2010; 6

41. Termine E, Michel GP. Transcriptome and secretome analyses of the adaptive response of Pseudomonas aeruginosa to suboptimal growth temperature. Int Microbiol. 2009; 12:7–12. [PubMed: 19440978]

42. von Tigerstrom RG, Stelmaschuk S. The use of Tween 20 in a sensitive turbidimetric assay of lipolytic enzymes. Can J Microbiol. 1989; 35:511–514. [PubMed: 2501015]

43. Vance RE, Rietsch A, Mekalanos JJ. Role of the type III secreted exoenzymes S, T, and Y in systemic spread of Pseudomonas aeruginosa PAO1 in vivo. Infection and immunity. 2005; 73:1706–1713. [PubMed: 15731071]

44. Mougous JD, et al. Identification, function and structure of the mycobacterial sulfotransferase that initiates sulfolipid-1 biosynthesis. Nature structural & molecular biology. 2004; 11:721–729.

45. Bligh EG, Dyer WJ. A rapid method of total lipid extraction and purification. Can J Biochem Physiol. 1959; 37:911–917. [PubMed: 13671378]

46. Brugger B, Erben G, Sandhoff R, Wieland FT, Lehmann WD. Quantitative analysis of biological membrane lipids at the low picomole level by nano-electrospray ionization tandem mass spectrometry. Proceedings of the National Academy of Sciences of the United States of America. 1997; 94:2339–2344. [PubMed: 9122196]

47. Devaiah SP, et al. Quantitative profiling of polar glycerolipid species from organs of wild-type Arabidopsis and a phospholipase Dalpha1 knockout mutant. Phytochemistry. 2006; 67:1907–1924. [PubMed: 16843506]

48. Welti R, et al. Profiling membrane lipids in plant stress response. J Biol Chem. 2002; 277:31994–32002. [PubMed: 12077151]
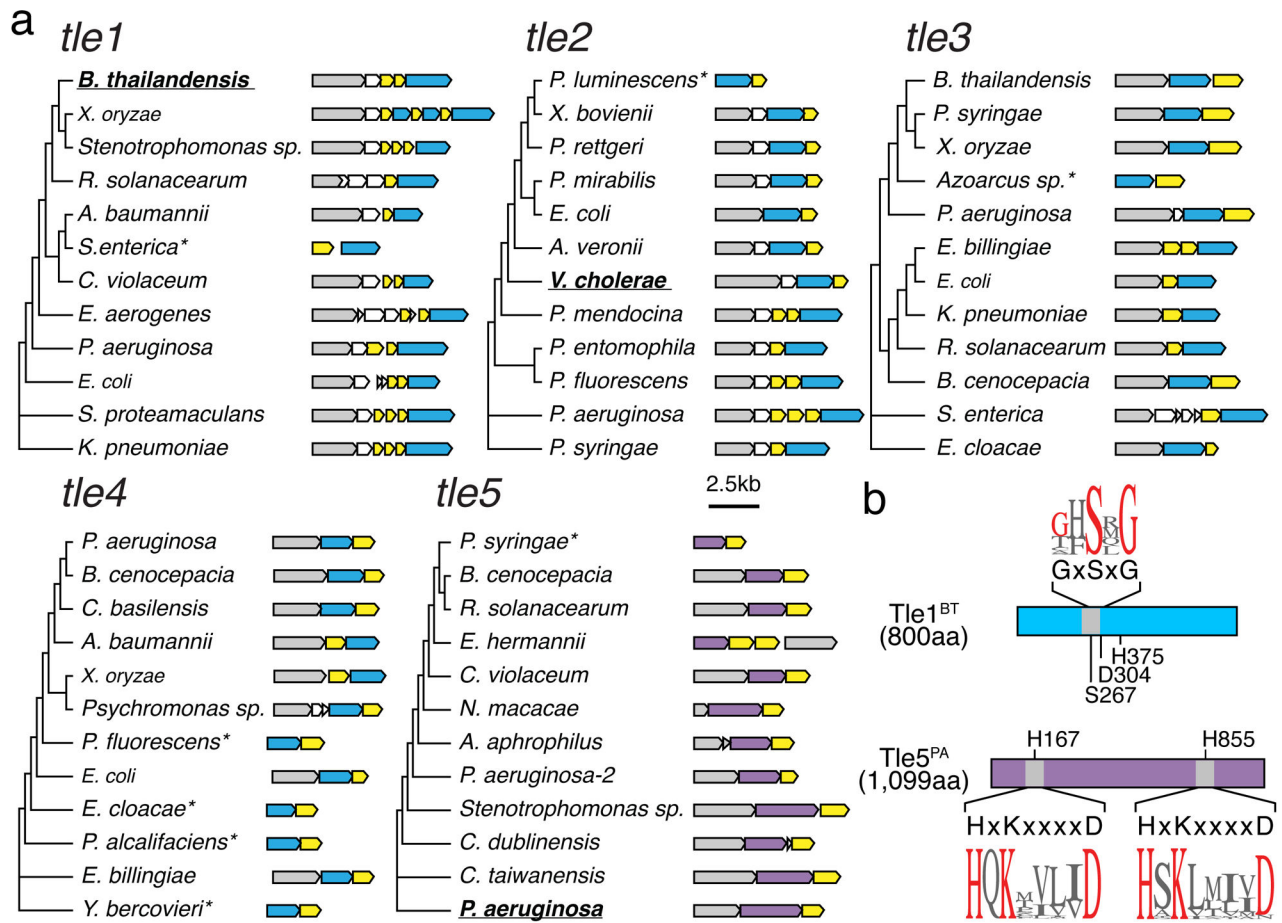
**Figure 1. Overview of the Tle superfamily**

**a,** Evolutionary trees, genetic organization, and phylogenetic distribution of select Tle family members. Genes are coloured by their predicted protein product (blue, Tle proteins with a GxSxG catalytic motif; purple, Tle proteins with dual HxKxxxxD catalytic motifs; grey, VgrG proteins; yellow, putative periplasmic immunity proteins). Branch lengths are not proportional to evolutionary distance. Asterisks denote *tle* genes without an apparent adjacent *vgrG* gene. **b,** Domain organization of a single member of the GxSxG and dual HxKxxxxD catalytic classes of Tle proteins. Regions comprising these catalytic motifs are labeled in grey, and positions of all putative catalytic residues are denoted. Sequence logos were generated from alignments of the catalytic motif from Tle1-4 (GxSxG) and catalytic motifs from Tle5 (HxKxxxxD).
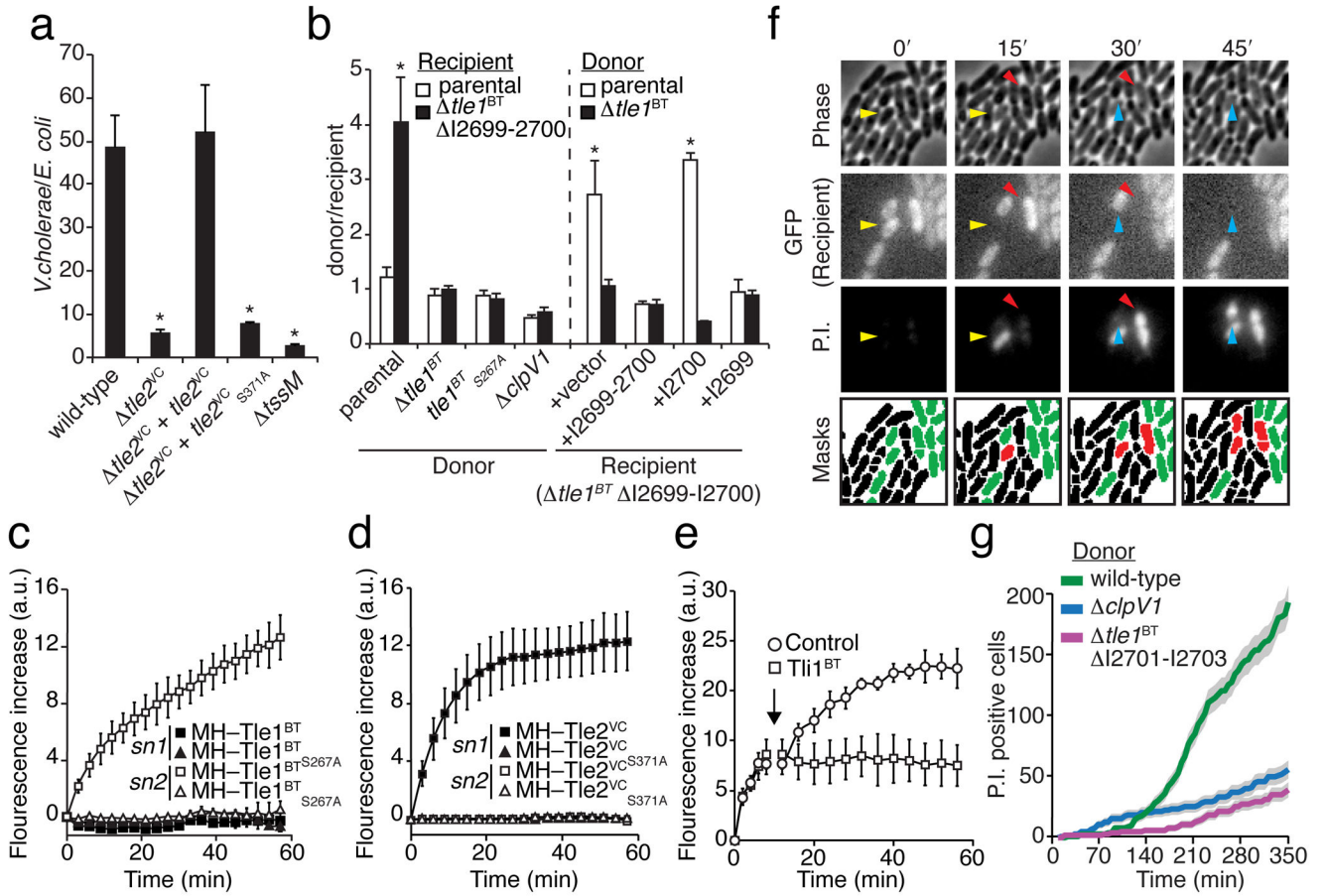
**Figure 2. Tle GxSxG-type proteins are antibacterial phospholipase effectors delivered by the T6SS**

Error bars for all panels ± s.d. **a,** Outcome of growth competitions between the indicated *V. cholera* strains and *E. coli*. The tssM strain is inactive for T6S. Asterisks denote competitive outcomes significantly different than those obtained with wild-type (P<0.05, n=3). **b,** Growth competition assays between the indicated *B. thailandensis* donor and recipient strains. The clpV1 strain is inactivated for T6SS-1, required for Tle1[BT] export[10]. The parental strain for all experiments in this panel is I2701-2703. Asterisks denote competition outcomes significantly different between indicated recipient strains (left) or indicated donor strains (right) (P<0.05, n=3). **c, d,** Enzymatic activity of the designated proteins against vesicles containing phospholipid derivatives with fluorescent moieties at the *sn1* or *sn2* positions (n=4). **e,** Enzymatic activity of MH–Tle1[BT] on *sn2*-labeled phospholipids as measured in (c) upon the addition of the indicated immunoprecipiate (arrow) (n=5). **f,** Representative cropped micrograph series displaying three propidium iodide (P.I.) uptake and subsequent lysis events in a growth competition experiment between *B. thailandensis* wild-type and a Tle1[BT]-sensitive recipient, I2698-I2703. Each event spans two frames and is highlighted by arrowheads. The mask frames depict cell assignments made by gating cells based on fluorescence (black, donor; green, recipient; red, P.I.-positive). **g,** Quantitation of P.I. staining events from *B. thailandensis* growth competitions
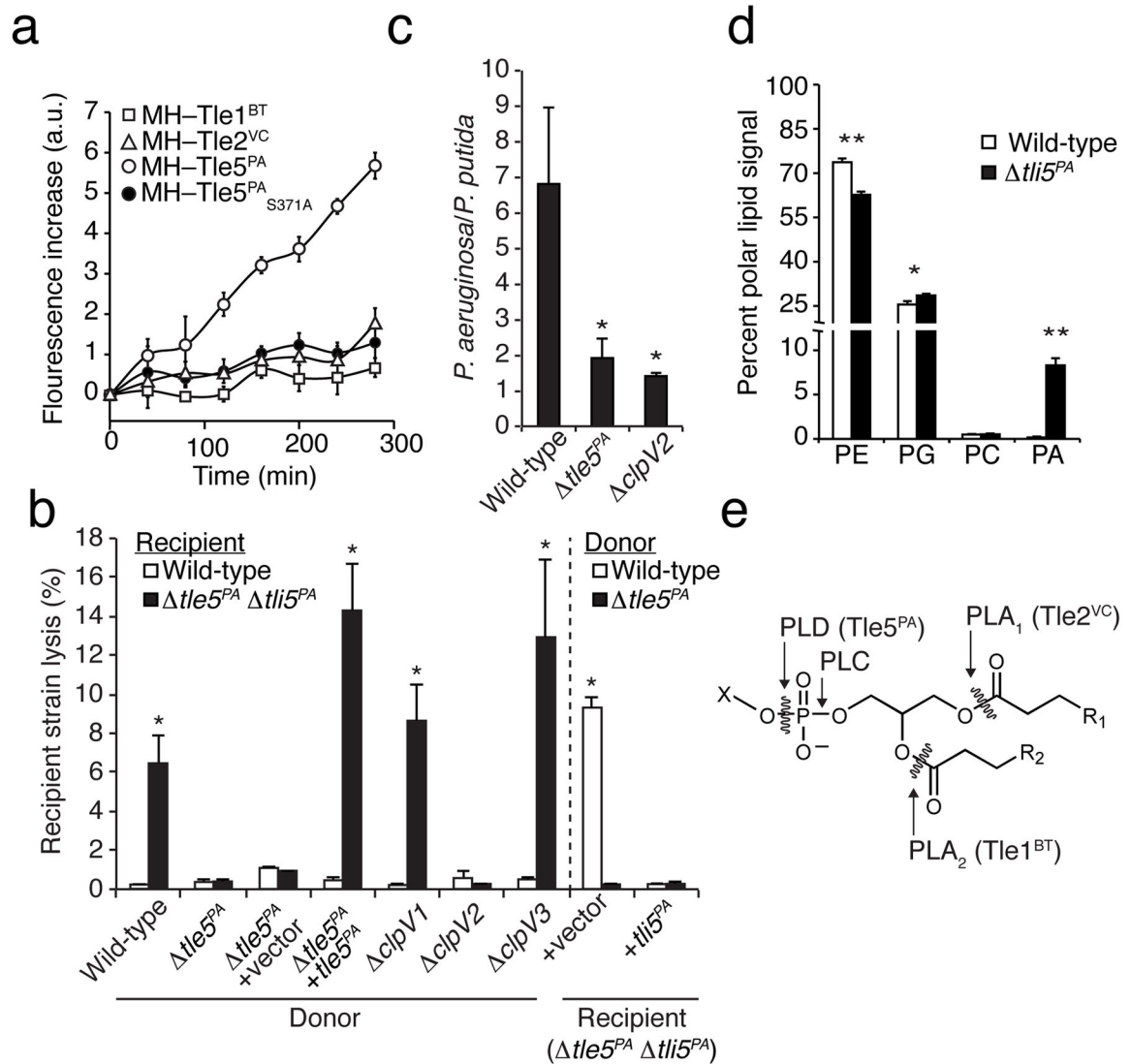
using automated custom software. The recipient strain was the same as used in (f). Shading indicates counting error.

**Figure 3. Tle5^PA is an HxKxxxxD-type interspecies antibacterial phospholipase effector delivered by the H2-T6SS of *P. aeruginosa***

Error bars for all panels ± s.d. **a,** PC-specific PLD activity of the indicated proteins against mixed lipid vesicles (n=3). **b,** Lysis of recipient strains grown in co-culture with the indicated donor strains. Asterisks mark experiments wherein recipient lysis is significantly different between indicated recipients (left), or between indicated donors (right) (P<0.05, n=3). c, Competitive growth of indicated *P. aeruginosa* strains against *P. putida* under T6SS-conducive conditions. Asterisks denote competition outcomes significantly different than those obtained with wild-type *P. aeruginosa* (P<0.05, n=3). **d,** Summary of phospholipid profiles of the indicated *P. aeruginosa* strains. Statistical significance noted (n=4, * P<0.01, ** P <0.001). **e,** Generalized schematic of a phospholipid indicating the activities defined in this study.